Structure of Isotropic Solutions of Rigid Macromolecules via Small-Angle Neutron Scattering: Poly(.gamma.-benzyl L-glutamate)/Deuterated Dimethylformamide

ARTICLE *in* MACROMOLECULES · JULY 1995

Impact Factor: 5.8 · DOI: 10.1021/ma00118a041

3 AUTHORS, INCLUDING:

Norman Joseph Wagner
University of Delaware
313 PUBLICATIONS **7,126** CITATIONS
SEE PROFILE

B. Hammouda
National Institute of Standards and Technology
121 PUBLICATIONS **2,396** CITATIONS
SEE PROFILE

Structure of Isotropic Solutions of Rigid Macromolecules via Small-Angle Neutron Scattering: Poly(γ-benzyl L-glutamate)/ Deuterated Dimethylformamide

Norman J. Wagner* and Lynn M. Walker

Department of Chemical Engineering, Colburn Laboratory, University of Delaware, Newark, Delaware 19716

Boualem Hammouda

NIST, Building 235, E151, Gaithersburg, Maryland 20899

Received July 8, 1994; Revised Manuscript Received February 22, 1995®

ABSTRACT: We have measured the structure factor for rigid-rod macromolecules in solution, poly(γ-benzyl L-glutamate) (PBLG) in deuterated dimethylformamide (d-DMF), in the isotropic phase. Small-angle neutron scattering measurements of a concentration series, from the dilute through the concentrated isotropic phase, have been analyzed using the recent modification of the random-phase approximation by Doi, Shimada, and Okano (DSO-RPA) for rodlike macromolecules, which includes nematic interactions. The results and comparison to theory are in good agreement with reported values from previous light scattering measurements performed by De Long and Russo at lower wave vectors. The concentrated isotropic phase exhibits an intensity increase that grows with increasing concentration, a pretransitional effect consistent with increased fluctuations in orientational order. Additional orientational fluctuation correlations are introduced into the theory through a phenomenological dependence of the excluded-volume parameter on the scattering wave vector, and good agreement with the measured scattering is found. Attempts to verify this behavior with lower molecular weight samples showed further anomalies.

I. Introduction

Fluids composed of rigid macromolecules are important in technologies using advanced materials such as high-performance fibers and liquid crystalline polymers (LCPs) and as nonlinear optical devices.[1] The performance of these materials often depends on the ability to control the alignment and order of the macromolecules during processing. Because of the large anisotropy of these molecules (the length-to-diameter ratios are on the order of 100), their alignment is strongly coupled to the flow field. Our ongoing research uses mechanical, optical, and neutron scattering measurements to determine the microstructure of model lyotropic liquid crystalline polymers.[2–4] To quantitatively model the flow alignment of LCPs, the physicochemical properties of rod geometry, persistence length, and nematic interaction strength must be determined.[5–7]

Scattering methods are a powerful means of determining these basic physicochemical properties.[8] The polymer of interest here is the rodlike macromolecule poly(γ-benzyl L-glutamate) (PBLG), which is an important model system that has received considerable attention. Indeed, substantial light scattering measurements have been performed on PBLG/DMF solutions by DeLong and Russo.[9] However, extracting the basic physicochemical properties from the scattering requires a detailed model linking the molecular order to the scattering. Recently, Doi, Shimada, and Okano[10–12] have derived an extension of the random-phase approximation (RPA) to include the effects of nematic interactions in the mean-field description of the molecular field. DeLong and Russo analyzed their light scattering results within this framework, finding good agreement for relatively dilute solutions but systematic deviations in the semidilute and concentrated isotropic regimes. To better understand these discrepancies, scattering using a different wavelength, such as neutrons instead of light, can provide additional information. In particular, for the molecular weights of interest here light scattering probes length scales on the order of the length of the rods ($qL \approx <1$), while small-angle neutron scattering (SANS) provides information from scattering wave vectors greater than the rod length ($qL \gg 1$).

In this paper, we report our findings for the determination of the excluded-volume and nematic potential parameters for PBLG in a helicogenic solvent, d-DMF, using small-angle neutron scattering (SANS). In what follows we discuss the experimental setup, sample preparation, and basic theoretical framework. After presenting the results and comparing with the DSO model, we attempt to account for the discrepancies by introducing a phenomenological description of pretransitional effects as scattering from orientational fluctuations, as characterized by a length-scale-dependent excluded volume. As a further test of this phenomenology, additional experimental results are then presented for shorter rods.

II. Experimental Section

Solutions of poly(γ-benzyl L-glutamate) (PBLG) (Sigma, M_ws 235 000 and 42 000) were prepared by drying and subsequent suspension into deuterated dimethylformamide (d-DMF). The reported average molecular weights were verified using capillary viscometry. The polymer was dried for a minimum of 24 h at 60 °C under vacuum before use and stored below 0 °C under nitrogen when dry. All samples were prepared and loaded into scattering cells under a nitrogen atmosphere to avoid water contamination. The solutions were allowed to equilibrate for at least 1 week before loading into 1-mm-thick quartz cells. Table 1 lists the details of the composition of the samples probed in this work.

In the helical state, the thermodynamic rod diameter (d) is 1.5 nm and the monomer length (L) 0.15 nm, with each monomer having a molecular weight of 219.[13] Thus, for our

* To whom correspondence should be addressed. E-mail: wagner@che.udel.edu.

® Abstract published in *Advance ACS Abstracts,* June 1, 1995.

0024-9297/95/2228-5075$09.00/0

Table 1. PBLG/d-DMF Samples

sample ID	PBLG, wt %	volume fraction (ϕ)	concn of PBLG (c) g/cm^3	c/c^*
		M_w = 235 000		
L(a)	0.56	0.005	0.006	0.052
L(b)	2.5	0.02	0.025	0.22
L(c)	4.4	0.036	0.046	0.40
L(d)	8.2	0.068	0.086	0.74
c^*	11	0.091	0.12	1.00
		M_w = 42 000		
S(a)	2.8	0.023	0.029	0.081
S(b)	22	0.19	0.24	0.67
S(c)	24	0.21	0.26	0.72
c^*	33	0.28	0.36	1.00

reported average molecular weights, the nominal rod lengths are 161 and 29 nm, respectively, giving L/d values of 107 and 19.

The last row in each section of Table 1 lists the critical concentration c^*, defined as the stability limit for the isotropic phase, needed in the DSO-RPA theory. Previous studies concerning the phase behavior of PBLG in DMF and other good solvents[14,15] indicate that the concentrations at the phase boundaries shift from Onsager-like behavior for shorter rod lengths (lower molecular weights) to Flory-like behavior for longer rods. As we cannot use the theoretical predictions for quantitative determination, we determine c^* from the experimentally observed phase behavior. The Onsager theory yields a prediction that $c^* = 0.89c_a$, where c_a is the nematic concentration at the isotropic–nematic phase boundary. The last column in Table 1 lists c/c^* as determined in this manner.

SANS experiments were performed on the NG3 SANS instrument at NIST. A wavelength of 6 Å and a velocity spread of 34.3% were used to provide the necessary flux, although additional experiments were performed at higher instrument resolution to verify results. The neutron scattering length densities for PBLG (3.60×10^{-14} cm^{-2}) and d-DMF (1.05×10^{-13} cm^{-2}) were calculated from the molecular structure. No exchange of deuterium and hydrogen on the PBLG was accounted for in the calculation. All data were absoluted by the standard procedures,[16] and circular averaging was performed to obtain the final $I(q)$ versus q data. Data at different detector distances were absoluted against the intensity measured at the 8 m distance, which was calibrated against known standards to obtain the absolute scale.

III. Theory

The scattering intensity in the Rayleigh–Gans–Debye approximation for rods at number density n with length L and diameter d is generally written as:

$$I(\mathbf{q}) = C\phi V_p(\Delta\varrho)^2\langle\sum_i^N\sum_j^N\int d\mathbf{r}_i\int d\mathbf{r}_j\, e^{i\mathbf{q}\cdot(\mathbf{r}_i-\mathbf{r}_j)}\rangle \quad (1)$$

where the sums are over all rods and $\mathbf{r}_i$ denotes the position of a material point within rod i, relative to the rod's center of mass $\mathbf{R}_i$, and $\langle\,\rangle$ denotes an ensemble average. In eq 1, $\mathbf{q}$ is the usual scattering vector. The factor C accounts for the sample thickness and instrument factors, and the volume fraction is defined as $\phi = n\pi Ld^2/4 = nV_p$. The scattering length density difference $\Delta\varrho$ gives the contrast between the rods and the solvent. The scattering can be separated into self-interacting and interacting terms as:

$$I(\mathbf{q}) = C\phi V_p(\Delta\varrho)^2\langle\sum_i^N F_i^2(\mathbf{q},\mathbf{u}_i) + \sum_i^N\sum_{j\neq i}^N\int d\mathbf{r}_i\int d\mathbf{r}_j\, e^{i\mathbf{q}\cdot(\mathbf{r}_i-\mathbf{r}_j)}\rangle \quad (2)$$

where $F_i(\mathbf{q},\mathbf{u}_i)$ is the form factor for the individual rod with orientation $\mathbf{u}_i$. For the special case of dilute rods, the scattering interference between rods is negligible and the integration can be performed for a single rod. Averaging over all N rods which have equal probability of orientation yields

$$I(q)_{(\text{dilute})} = C\phi V_p(\Delta\varrho)^2\langle F^2(q)\rangle \quad (3)$$

This defines the scattering form factor $\langle F^2(q)\rangle$ for isotropically distributed rods. This form factor can be calculated for long rods directly from relations given in van de Hulst.[8] The result of such a calculation for rods of length L that are randomly distributed with respect to orientation is

$$\langle F^2(q)\rangle = \frac{2}{qL}\int_0^{qL}\frac{\sin(\omega)}{\omega}\,d\omega - \left(\frac{\sin(qL/2)}{qL/2}\right)^2 \quad (4)$$

For interacting rods, the integrations depend upon the relative rod orientation and position, which are coupled even in a macroscopically isotropic solution. For macroscopically isotropic solutions of rodlike macromolecules the scattering is isotropic, and it is, therefore, often convenient to define an effective structure factor (as is done for spherical particles)

$$I(q) = C\phi V_p(\Delta\varrho)^2\langle F^2(q)\rangle S_{\text{eff}}(q) \quad (5)$$

where $S_{\text{eff}}(q)$ accounts for all of the correlations between rods, including orientational fluctuations not accounted for in the form factor.

To simplify the analysis, the following assumptions are often made in the literature:[17]

(1) The orientation of a rod is decoupled from all other rods, except for a mean-field orientational contribution, for all separations.

(2) The center of mass pair correlation depends only on the relative distance ($r = |\mathbf{r}_i - \mathbf{r}_j|$) of separation.

(3) The particles are monodisperse in shape and scattering length density.

This rigorously yields

$$I(q) = C\phi V_p(\Delta\varrho)^2[\langle F^2(\mathbf{q})\rangle + \langle F(\mathbf{q})\rangle^2 h(\mathbf{q})] \quad (6)$$

where $h(\mathbf{q})$ describes the rod center of mass correlations. This equation, which defines $S_{\text{eff}}(q)$, has found utility in the analysis of scattering from low aspect ratio systems[17,18] and has been verified for this system in the nematic phase.[3]

The recent theory of Doi, Shimada, and Okano (DSO)[10–12] applies the random-phase approximation (RPA) to calculate the structure factor of wormlike macromolecules in solution. In the RPA, the chain segments experience a molecular field due to interactions with other chain segments, which is written in terms of a mean-field potential. This mean-field potential is determined by a self-consistent calculation of the segmental concentration fluctuations. The DSO model extends this mean-field calculation beyond simple excluded-volume contributions to include the effects of nematic interactions. The ensuing self-consistent determination of the mean field is expected to become more exact in the limit of infinitely long, rigid-rod polymers. The major approximations involve expanding the orientationally dependent molecular field in spherical harmonics and retaining only the first (excluded-volume) and second (nematic interaction) terms.[19]

The results of their calculations are summarized for monodisperse, rodlike polymers below, where the original notation of DSO has been maintained except for the straightforward nondimensionalization and the definition of $S_{eff}(q)$:

$$S_{eff}(q) = \frac{1 + R_0/P_0}{1 + \gamma_0(P_0 + R_0)} \tag{7}$$

where

$$R_0(q) = \frac{2\gamma_1 S_0^2}{3[1 - \gamma_1 T_0]}$$

$$P_0(q) = \int_0^1 dx \left[\frac{\sin(qx)}{qx}\right]^2$$

$$S_0(q) = \frac{3}{2}\int_0^1 dx \left[\frac{\sin(qx)}{qx}\right]^2 \left(x^2 - \frac{1}{3}\right)$$

$$T_0(q) = \frac{3}{2}\int_0^1 dx \left[\frac{\sin(qx)}{(qx)}\right]^2 \left(x^2 - \frac{1}{3}\right)^2 \tag{8}$$

Note that the function $P_0(q) = \langle F^2(q)\rangle$ is the form factor, defined previously. The function $R_0(q)$ is a direct result of the nematic interaction, as characterized by the strength γ_1. This function diverges when $\gamma_1 T_0(q) = 1$, a criterion for the limit of stability of the isotropic phase. Note that as $\gamma_1 \to 0$ the model reduces to the standard RPA results. The excluded-volume parameter γ_0 and the nematic interaction strength are related to the parameters in the DSO papers by (where n is the concentration in rods per unit volume and L is the rod length):

$$\gamma_0 = nL\nu_0 \tag{9}$$

$$\gamma_1 = nL\nu_1 \tag{10}$$

The excluded-volume parameter can be directly calculated from the rod geometry, as done by Onsager.[20] It is related to the second virial coefficient A_2 through[9,21]

$$\gamma_0 = 2nMA_2 \tag{11}$$

where M is the molecular weight. The second virial coefficient has been calculated for long, rigid cylinders as

$$A_2 = \pi N_A d L^2/4M^2 \tag{12}$$

Since L is proportional to molecular weight, the second virial coefficient is independent of molecular weight. For our system, the value of A_2 is calculated to be 3.33×10^{-4} cm^3 mol·g^{-2}. DeLong and Russo[9] measured A_2 for a similar sample of PBLG/DMF using light scattering and found good agreement with the calculated values.

The nematic interaction parameter γ_1 is responsible for the loss of stability of the isotropic phase. In this manner, it is possible to relate γ_1 directly to this critical concentration c^*. In the DSO model, this becomes

$$\gamma_1 = 2c/15c^* \tag{13}$$

IV. Results and Discussion

The excluded volume and the strength of the nematic interaction parameter are determined by fitting the DSO model to plots of absolute scattering intensity.

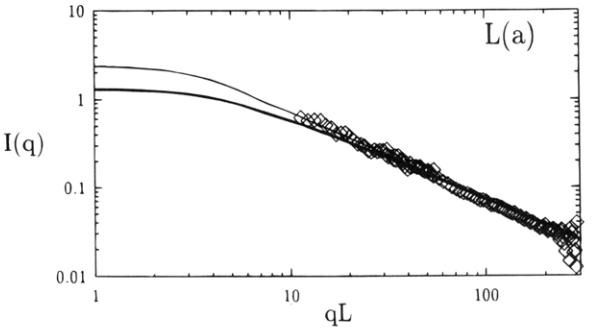

Figure 1. SANS intensity (units, cm^{-1}) for system L(a) (◇) versus qL: (—) form factor fit; (thick line) predicted fit.

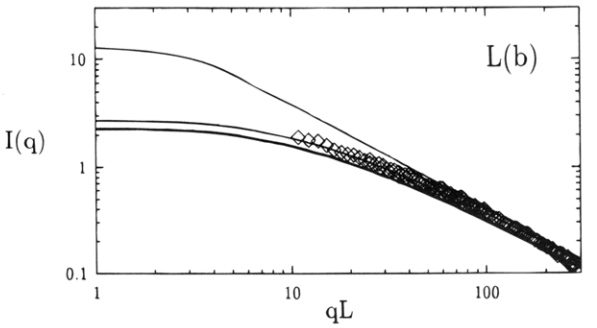

Figure 2. SANS intensity (units, cm^{-1}) for system L(b) (◇) versus qL. The fits correspond to a (thin line) form factor fit, (thick line) a predicted fit, and (middle line) an optimized fit.

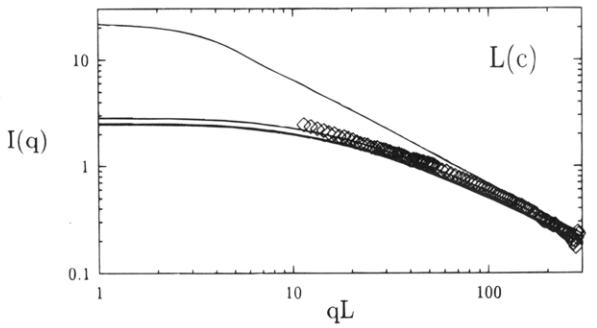

Figure 3. SANS intensity (units, cm^{-1}) for system L(c) (◇) versus qL. The fits correspond to (thin line) a form factor fit, (thick line) a predicted fit, and (middle line) an optimized fit.

Previous light scattering measurements by DeLong and Russo[9] determined values for the second virial coefficient from the variation of the low qL scattering intensity versus scattering angle; thus, our measurements complement their work. Our results for the high molecular weight system (L(a–d)) listed in Table 1 are shown in Figures 1–4; all four data sets eventually are limited to the expected q^{-1} behavior at large qL. From the slopes, we verified the scattering length density difference (see Figure 5a). The range of scattering vectors is smaller than the point where correlations from the internal structure of the rod (on the order of the rod diameter) would begin to appear ($\approx\pi(L/d)$); hence, the thin rod form factor should be appropriate throughout. The slope at large qL yields the prefactor times π; thus, a plot of these slopes against the respective volume fractions of the rods should have a slope of $\pi V_p(\Delta\varrho)^2$. As seen in Figure 5b, these points lie along a line through the origin of slope 500π cm^{-1}, in good agreement with the calculated slope of 480π cm^{-1}. The values of $A = \phi V_p(\Delta\varrho)^2$ are given in Table 2 for reference.

Calculations of the absolute scattering intensity using the RPA model and the experimentally verified prefac-

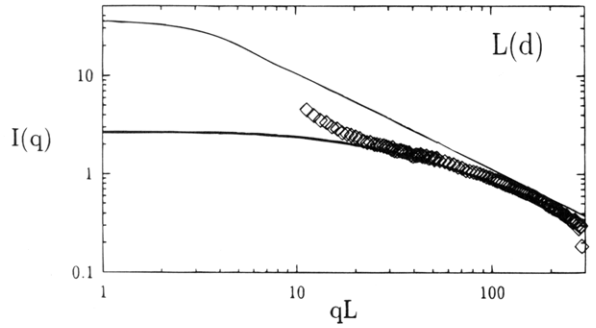

Figure 4. SANS intensity (units, cm^{-1}) for system L(d) (◇) versus qL. The fits correspond to (thin line) a form factor fit and (thick line) a predicted fit.

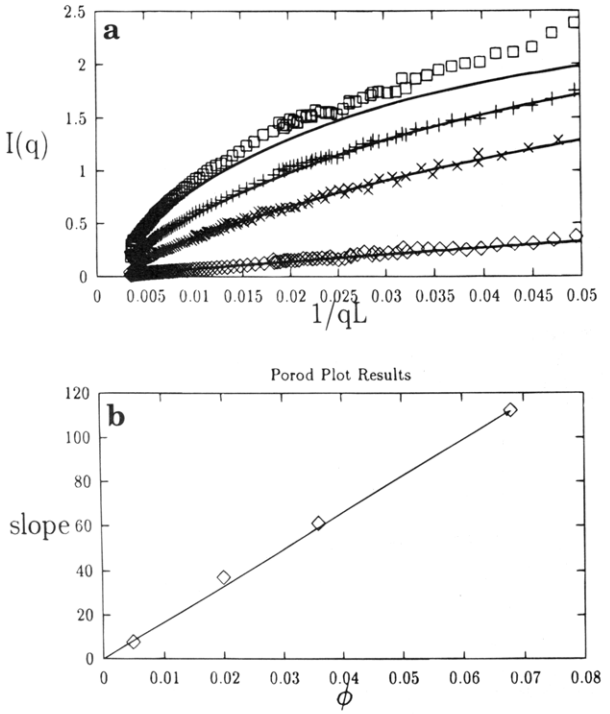

Figure 5. (a) Porod plots for systems L(a)−(d), bottom to top, respectively. (b) Porod plot results (◇) and best fit line.

Table 2. Fit Parameters

sample code	A (cm^{-1}) predicted	A (cm^{-1}) measured	γ_0 predicted	γ_0 measured	$15/2\gamma_1$	ξ
L(a)	2.4	2.4	0.84	0	0.052	
L(b)	11	13	3.8	3.8	0.22	
L(c)	19	22	6.7	6.7	0.46	0.15
L(d)	36	36	12	12	0.74	0.07
S(a)	2.2	2.5	0.76	1.2	0.081	
S(b)	18	11	6.2	6.2	0.67	
S(c)	20	14	6.9	6.9	0.72	

tors are compared to experimental data in Figures 1−4. The dilute sample L(a) is fit accurately with the form factor, verifying the rod length of $L = 161$ nm. For the higher concentrations, the three model lines represent the RPA fit using the theoretical values for the excluded-volume parameter, the RPA fit optimized to fit the intensity, and simply the isotropic form factor (times the appropriate prefactor) for reference. In all of these fits, the nematic interaction parameter was kept at its predicted value of $\gamma_1 = 2c/15c^*$ as the results were insensitive to moderate variations in γ_1. The values for the excluded-volume parameter and the nematic interaction parameter are given in Table 2. The optimum excluded volume and nematic interaction parameters

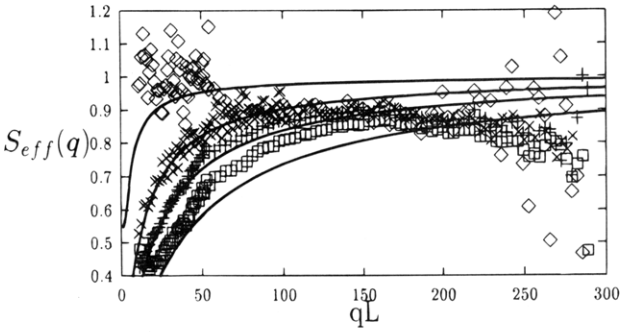

Figure 6. $S_{eff}(q)$: (◇) system L(a), (×) system L(b), (+) system L(c), (□) system L(d) for optimal DSO fits (thick lines).

and the quality of the RPA fit for the entire range of qL probed are close to the calculated values for the samples of lower concentration. Similar behavior was reported by DeLong and Russo,[9] where the low qL intensity was well fit by the predicted RPA parameters for $c/c^* \leq \approx 0.3$.

There is some evidence of a correlation peak in the intensity for samples L(c) and L(d), as seen as a positive deviation from theory at lower qL in the plot of $S_{eff}(q) = I(q)/(A\langle F^2(q)\rangle)$ shown as Figure 6 (more clearly seen as the upturn in Figures 3 and 4). This method of comparing the data and experiment is much more stringent across the entire range of scattering vectors probed, although it does emphasize the low-intensity data taken at large qL. The small deviations at higher values of scattering vector are not significant as polydispersity and instrument broadening effects have not been taken into account (although neither can introduce extrema into the intensity, they can distort the curvature slightly). The data for the form factor (L(a)) are scattered about 1 as expected, while the data for samples L(c) and L(d) show upturns at lower qL and are systematically higher than the predicted values, with a broad extremum in the deviation near $qL \approx 100$. The RPA model predicts the monotonic increase with qL observed for samples L(a) and L(b) but cannot account for the increased intensity seen around $qL \leq \approx 20$ nor $qL \approx 100$ for both samples L(c) and L(d).

In the concentration range probed by these experiments the RPA predictions are insensitive to reasonable variations in the nematic parameter γ_1, being dominated by the excluded-volume parameter γ_0. Given the above results, the validity of the RPA appears to be limited to $c/c^* \leq \approx 0.3$. As the large qL data probed here are not sensitive to the choice of the nematic interaction parameter, we cannot determine the validity of the DSO extension in the lower concentration regime. However, the significant deviations at values of $qL \approx 20$ for $c/c^* > 0.3$ (samples L(c) and L(d)) cannot even qualitatively be accounted for by the DSO-RPA model.

These SANS data suggest that fits of the low qL data from light scattering would show significant deviations from the DSO predictions. This was seen by DeLong and Russo for all of their molecular weights, where the excluded-volume parameter appears to saturate at $c/c^* \approx 1/3$. Sample aggregation was ruled out, and depolarized light scattering suggested that there are orientational correlations present at these concentrations and above. These pretransitional effects, which were earlier pictured as clusters of rods with local orientational ordering (termed "swarms"), are more appropriately conceptualized as continuous variations in the spatial correlations in the local degree of orientational order.[7] The manifestation of such orientational fluctuations upon the thermodynamics of rod solutions would be to

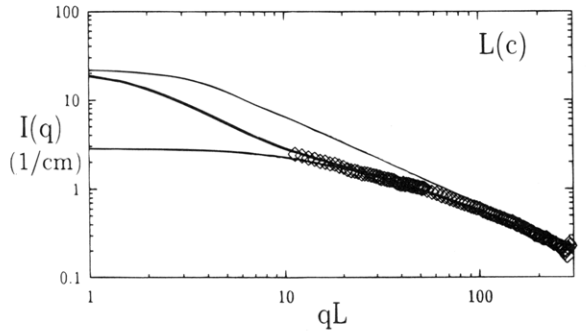

Figure 7. SANS intensity (units, cm^{-1}) for system L(c) (◇) versus qL. The fits correspond to (thin line) a form factor fit, (lower line) an optimized DSO fit, and (thick line) an extended DSO with $\xi = 0.15$.

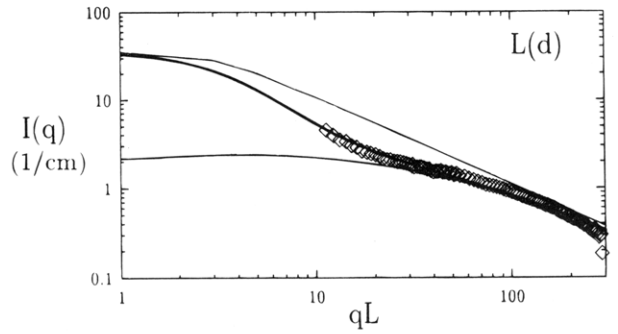

Figure 8. SANS intensity (units, cm^{-1}) for system L(d) (◇) versus qL. The fits correspond to (thin line) a form factor fit, (lower line) an optimized DSO fit, and (thick line) an extended DSO with $\xi = 0.07$.

effectively reduce the magnitude of the excluded volume over some correlation length. In fact, Maeda,[22] in a matrix formulation of the dynamic DSO model, also invokes a length-scale dependence to the osmotic virial coefficient so it becomes a function of qL. This is necessary to explain the measured decrease in the apparent mutual diffusion coefficient with increasing concentration seen in solutions of this polymer.[23]

Such orientational ordering would also produce an increased scattering intensity in the region about $qL \approx 100$. As a thought experiment, consider packing the rods into a perfect columnar phase at the volume fractions used. The inter-rod correlation length would be given by $qL = 2\pi\sqrt{\phi}(L/d)$, which is about $qL \approx 100-200$ and would manifest itself in the experiments as a positive deviation from the RPA prediction. This is evident in Figure 6 for both samples L(c) and L(d).

The upturn at $qL \approx 20$ suggests possible center-of-mass or orientation-position correlations. Currently there is no theoretical development available capable of predicting such correlations in this concentrated isotropic regime. Unlike the success that perturbation theories enjoy when applied to charged rod systems,[24-27] the large L/d ratio and the high concentration of our system (relative to $1/L^3$) yield aphysical results when mappings to effective spherical particles are used.

We can try to estimate this effect by introducing a length-scale dependence to the excluded-volume parameter. As a *phenomenological model* inspired by the physical picture of orientation fluctuations, we anticipate that there is a length-scale dependence to the excluded volume. When two rods are close together in a *concentrated*, isotropic solution, the excluded-volume parameter should be significantly lower for that pair of rods because they must be locally aligned to permit such a relatively high packing density (relative to 1 rod per every L^3 of volume). Empirically, the high qL scattering should still be influenced to a large degree by the rotationally averaged excluded volume, as evidenced by the good agreement between experiment and theory at large qL. The introduction of a new length scale must satisfy momentum conservation; without further theoretical justification we introduce a wavelength-dependent excluded-volume parameter as:

$$\gamma_0'(qL) = \gamma_0 \frac{(\xi qL)^2}{1 + (\xi qL)^2} \tag{14}$$

where ξ is some measure of the scale of the correlation length for the excluded volume.

Figures 7–9 demonstrate the ability to account for

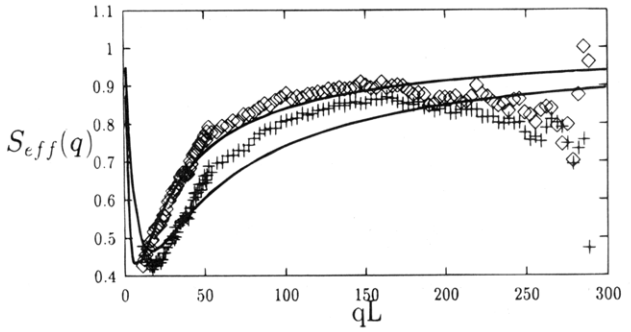

Figure 9. S_{eff} for optimal modified DSO fits, systems L(c) (◇) and L(d) (+), and extended DSO fits (—).

the upturn at low qL for both samples L(c) and L(d) without varying any of the original best-fit parameters. The best-fit values for this new parameter ξ are 0.1 and 0.07, respectively. The trend is as expected; i.e., approaching the isotropic–nematic transition leads to greater orientation fluctuations and, thus, to a lowering of the excluded volume relative to the rotationally averaged value (at fixed qL). However, the c/c^* value at which this first manifests itself is surprisingly low. Recent flow birefringence measurements also detect flow-induced pretransitional ordering at low concentrations[28] for (hydroxypropyl)cellulose in water, and similar pretransitional effects have also been observed for PBLG solutions using flow birefringence and rheology.[29]

This simple model also predicts that the scattering intensity at zero wave vector should be significantly higher for samples in the concentrated isotropic regime. The scattering correlation length ζ, defined as

$$I(0)/I(q) = 1 + q^2\zeta^2 + Dq^4 + \ldots \tag{15}$$

is given in the DSO model by

$$(L/6\zeta)^2 = 1 + \gamma_0 \tag{16}$$

Note that the dependence on rod length is scaled out, and the correlation length is purely a function of the total excluded volume of the rods as characterized by the parameter γ_0. As seen in eq 14 for a finite value of ξ, $\gamma_0 \to 0$ as $(qL)^2$ for small scattering angles. Thus, the prediction of this modification of the DSO model is that

$$(L/6\zeta)^2 \to 1 \tag{17}$$

Indeed, DeLong and Russo report that values of this scattering correlation length are well described by the

DSO model (eq 16) until γ_0 of about 3. Then, there is a general, but erratic, tendency for the correlation length to return to a value of 1, as predicted by the modification. This downturn cannot be explained by the nematic interaction terms, as they enter in at the q^4 term. Thus, our phenomenological modification of the DSO model is also consistent with earlier light scattering measurements of the correlation length at low values of qL.

PBLG is thought to be a model, hard-rod-like sample,[30] yet weak molecular attractions between rods may exist. Therefore, we cannot rule out the possibility that the upturn at low qL is due to weak attractive forces that first manifest themselves in the semidilute regime. This would be consistent with dispersion forces, for example. However, the evidence that the dilute solutions do not aggregate supports the notion that discrepancies between the scattering curves and the DSO predictions are a consequence of orientational correlations not adequately represented in the theory. Attractive interactions could, in principle, be detected from the temperature sensitivity of the structure. In practice, however, the rod stiffness and solubility in the solvent are also affected by temperature, complicating interpretation of the results.

Small amounts of water contamination aggregates PBLG in DMF. During the course of our experiments we noticed no visible signs of aggregation and took the necessary precautions to eliminate sample exposure to water. Further, the scattering curves were found to be reproducible over the duration of 6 months for samples properly sealed and stored. We did investigate a sample that had been exposed to air and showed visible signs of weak aggregation (cloudiness and thickening). The resulting SANS scattering curve showed an increased intensity of many orders of magnitude at low scattering vector, presumably due to the formation of large aggregates. Therefore, although we cannot unequivocally discount weak attractions, we can state to the best of our abilities that the samples were not aggregated due to water contamination.

To further test this idea of scattering from orientational fluctuations associated with pretransitional effects, we performed similar scattering experiments on a lower molecular weight sample (systems S(a−c); Table 1). The experimental design was to probe lower effective qL values by shortening L (by lowering the molecular weight). Given $L/d \approx 19$, the sample exhibited an onset of the biphasic regime at $c_i \approx 32$ g/cm^3, which is between the Onsager value of 21 g/cm^3 and the Flory prediction of 46 g/cm^3.[14] No form factor measurements were made because of the reduced scattering intensity of these shorter rods and the increased incoherent scattering from the higher concentration of hydrogen (from the polymer).

A composite of the scattering curves is shown in Figure 10, along with the predicted values based on the DSO model (with the parameter values listed in Table 2). The dilute sample is in good agreement with the DSO-RPA model, as expected from the higher molecular weight data ($c/c^* < 0.3$). However, the scattering measured for the two higher concentrations falls significantly *below* the predicted curves, which is opposite from the higher molecular weight sample. Thus, the phenomenological correction for nematic interactions was not testable. Interestingly, the data show an intensity maximum with concentration in the isotropic phase, which is not predicted by the DSO-RPA theory. One possible source of this anomalous behavior is the

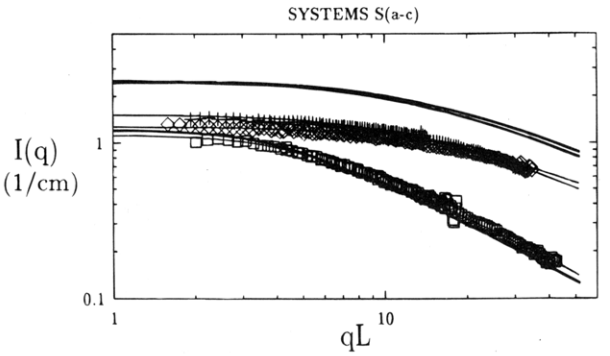

Figure 10. $I(q)$ versus qL for systems S(a) (□), S(b) (+), and S(c) (◇). The thick lines are the DSO predictions; the thin lines are the best fits.

increased turbidity (the transmissions where 65−70% for samples S(c) and S(d), whereas all other samples had transmissions above 80%) due to higher incoherent scattering, although this should not change the qualitative scattering behavior. This seemingly anomalous behavior is, however, consistent with the observations of DeLong and Russo, who found anomalous behavior for the virial coefficient for a similar molecular weight[9] (they cite polydispersity as a possible source of the discrepancy). Thus, these shorter rod experiments failed to corroborate the observations seen for the higher molecular weight samples at high concentrations but do support the applicability of the DSO-RPA model in the more dilute regimes.

V. Conclusions

In conclusion, we have found that the RPA model gives good predictions for the observed SANS scattering from PBLG rods in d-DMF in the dilute and semidilute isotropic concentrations ($c/c^* \leq 0.3$). However, at higher relative concentrations, correlations are evident in the scattering that cannot be predicted by the random-phase approach. We find that the extension of the RPA approach to include the nematic interactions has little effect on the predictions for the range of qL probed in this work. Rather, the excluded-volume parameter must be modified to account for the length-scale dependence of the nematic interaction.

Although the RPA model becomes exact in the limit of infinite rigid rods, in the DSO solution it is assumed that the molecular field can be separated into excluded-volume and interaction terms with constant strength. However, it is clear from our phenomenological fit, which accounts presumably for the effects of orientation fluctuations on the excluded volume, that in the concentrated isotropic regime the excluded-volume parameter itself must reflect the strength of the local nematic potential acting to align the rods. If one accounts for the dependence of the excluded volume upon the local orientation of the rods, such as is done by Onsager[20] in the derivation of the overlap volume for hard rods, the excluded-volume parameter will no longer be a constant in the concentrated isotropic regime but rather a function of the scattering vector. We have introduced a phenomenological coefficient capable of explaining the major discrepancy between the DSO model and our scattering data, which yields qualitatively good predictions for the correlation length, as measured in previous light scattering studies. However, this phenomenology remains to be justified by more rigorous theoretical or computational studies.

Acknowledgment. Support for this project from the National Science Foundation (CTS-9158146), DuPont Polymers, and the Delaware Research Partnership is greatfully acknowledged. SANS measurements were performed on the NIST NG3 30-m instrument, which supported by NSF under Grant No. DMR-9122444. Certain equipment and instruments or materials are identified in this paper in order to adequately specify the experimental conditions. Such identification does not imply recommendation by the National Institute of Standards and Technology, nor does it imply that the materials are necessarily the best available for the purpose.

References and Notes

(1) Commission on Engineering National Research Council, National Materials Advisory Board and Technical Systems. *Liquid Crystalline Polymers*; National Academy Press: Alexandria, VA, 1990.
(2) Walker, L. M.; Wagner, N. J. *J. Rheol.* **1994**, *38* (5), 1525.
(3) Wagner, N. J.; Walker, L. M. *Macromolecules* **1994**, *27*, 5979.
(4) Walker, L. M.; Wagner, N. J.; Larson, R.; Mirau, P.; Moldenaers, P. *J. Rheol.*, submitted.
(5) Larson, R. *Constitutive Equations for Polymer Melts and Solutions*; Butterworths: New York, 1988.
(6) Doi, M.; Edwards, S. F. *The Theory of Polymer Dynamics*; Clarendon Press: Oxford, 1986.
(7) de Gennes, P.-G.; Prost, J. *The Physics of Liquid Crystals*, 2nd ed.; Clarendon Press: Oxford, 1993.
(8) van de Hulst, H. C. *Light Scattering by Small Particles*; Dover: New York, 1957.
(9) DeLong, L. M.; Russo, P. S. *Macromolecules* **1991**, *24*, 6139.
(10) Doi, T.; Shimada, M.; Okano, K. *J. Chem. Phys.* **1988**, *88*, 4070.
(11) Shimada, M.; Doi, T.; Okano, K. *J. Chem. Phys.* **1988**, *88*, 2815.
(12) Shimada, M.; Doi, T.; Okano, K. *J. Chem. Phys.* **1988**, *88*, 7181.
(13) Block, H. *PBLG and other glutamic acid forming polymers*; Gordon and Breach: New York, 1983.
(14) Kubo, K.; Ogino, K. *Mol. Cryst. Liq. Cryst.* **1979**, *53*, 207.
(15) Baek, S. G.; Magda, J. J.; Larson, R. G. *J. Rheol.* **1993**, *37*, 1201.
(16) Barker, J.; Krueger, S.; Hammouda, B. *SANS Manuals*; NIST: Gaithersburg, MD, 1993.
(17) Kalus, J.; Hoffmann, H.; Ibel, K. *Colloid Polym. Sci.* **1989**, *267*, 818.
(18) Cummins, P. G.; Staples, E.; Hayter, J. B.; Penfold, J. *J. Chem. Soc., Faraday Trans. 1* **1987**, *83*, 2773.
(19) Hammouda, B. *J. Chem. Phys.* **1993**, *98* (4), 3439.
(20) Onsager, L. *Ann. N.Y. Acad. Sci.* **1949**, *51*, 627.
(21) Yamakawa, H. *Modern Theory of Polymer Solutions*; Harper and Row: New York 1971; Appendix IVA.
(22) Maeda, T. *Macromolecules* **1989**, *22*, 1881.
(23) Russo, P. S.; Karasz, F. E.; Langley, K. H. *J. Chem. Phys.* **1984**, *80*, 5312.
(24) Canessa, E.; D'Aguanno, B.; Weyerich, B.; Klein, R. *Mol. Phys.* **1981**, *73*, 175.
(25) Schneider, J.; Hess, W.; Klein, R. *J. Phys. A: Math. Gen.* **1985**, *18*, 1221.
(26) Schneider, J.; Hess, W.; Klein, R. *Macromolecules* **1986**, *19*, 1729.
(27) Schumacher, G. A.; van den Ven, T. G. M. *Faraday Discuss. Chem. Soc.* **1987**, *83*, 75.
(28) Edwards, B. J.; McHugh, A. J. *J. Rheol.* **1993**, *37* (4), 743.
(29) Mead, D. W.; Larson, R. G. *Macromolecules* **1990**, *23*, 2223.
(30) Helfrich, J.; Hentschke, R.; Apel, U. M. *Macromolecules* **1994**, *27*, 472.

MA946295G